

## A compressional study of MgSiO<sub>3</sub> orthoenstatite up to 8.5 GPa

DEMELZA A. HUGH-JONES, ROSS J. ANGEL

Department of Geological Sciences, University College London, Gower Street, London WC1E 6BT, U.K.

### ABSTRACT

A single crystal of MgSiO<sub>3</sub> orthoenstatite has been studied by single-crystal X-ray diffraction in a diamond-anvil cell up to a pressure of 8.5 GPa. From the unit-cell data, it has been shown that the volume variation with pressure is best described by two independent equations of state, with significantly different values for their room-pressure bulk modulus,  $K_0$ , and its first derivative,  $K'_0$ : at  $P < 4$  GPa,  $K_0 = 95.8(3.0)$  GPa, and  $K'_0 = 14.9(2.0)$ ; at  $P > 4$  GPa,  $K_0 = 122.8(16.5)$  GPa, and  $K'_0 = 5.6(2.9)$ .

A series of structural refinements carried out at pressure intervals of  $\sim 1$  GPa shows that there is a change in compression mechanism at about 4 GPa that would account for this break in the equation of state of the pyroxene. Below 4 GPa the SiO<sub>4</sub> tetrahedra are essentially incompressible, with no change in Si-O bond lengths and O-Si-O bond angles, whereas at higher pressures the Si-O bond lengths shorten in a regular way, with no angular distortion of the SiO<sub>4</sub> tetrahedra. The linear volume compressibility of both of the tetrahedra between 4 and 8 GPa is  $0.0062(1)$  GPa<sup>-1</sup> [corresponding to a bulk modulus of  $162(3)$  GPa]. By contrast, the Mg-O bond lengths decrease steadily over the whole pressure range studied; the compression of each of the MgO<sub>6</sub> octahedra may be described by a single third-order Birch-Murnaghan equation of state: for the M1 site,  $K_0 = 53.2(5.4)$  GPa, and  $K'_0 = 31.9(6.3)$ ; for the M2 site,  $K_0 = 63.1(8.5)$  GPa, and  $K'_0 = 26.7(7.9)$ .

There is a well-defined change in both the degree of kinking of the tetrahedral chains (as measured by changes in the O3-O3-O3 chain extension angle) and the amount of tetrahedral tilt toward the (100) plane at about 4 GPa. At low pressures the B chain, which is more distorted at room pressure, kinks dramatically while keeping the bases of its tetrahedra at a constant orientation of approximately 7° from the (100) plane, whereas above  $\sim 4$  GPa the kinking ceases, and the tetrahedra begin to tilt steadily toward the (100) plane. The A chain behaves essentially in the reverse way: below 4 GPa the tetrahedra tilt markedly toward the (100) plane with only a little chain kinking occurring, whereas at higher pressures, the tetrahedral tilt virtually stops, and the kinking continues slowly in the opposite direction.

### INTRODUCTION

Pyroxenes are major components of the Earth's upper mantle; the transformation of these chain silicates to higher density garnets is a possible contribution to the seismic discontinuity that divides the upper mantle from the transition zone at about 400 km (Gasparik, 1989). At depths shallower than 400 km, two separate pyroxene phases are stable—a diopside-jadeite solid solution that contains the Na and Ca components, and a Ca-poor pyroxene with an approximate formula of (Mg,Fe)SiO<sub>3</sub>. Much work has already been done on the phase transitions between orthorhombic and monoclinic pyroxenes of several compositions at both high temperature and pressure, and the general topology of the MgSiO<sub>3</sub> enstatite phase diagram has been determined by Angel et al. (1992a). At high pressures and temperatures, orthoenstatite transforms to a monoclinic (C2/c) structure (Pacalo and Gasparik, 1990; Kanzaki, 1991). This clinoenstatite polymorph is the stable high-pressure phase of MgSiO<sub>3</sub>,

enstatite. The  $\Delta V$  for this transition has previously been estimated at  $\sim 3\%$ , and it has been suggested (Angel et al., 1992a) that the orthorhombic to monoclinic C2/c enstatite transition may contribute to the Lehmann seismic discontinuity at depths of 180–280 km in the subcontinental mantle. In order to assess the contributions of the enstatite component to the seismic structure of the upper mantle, it is important to measure the equations of state of the individual enstatite polymorphs in situ at high pressures, to determine not only their densities at depth but also the  $\Delta V$  across the various phase boundaries.

Raman experiments carried out on an MgSiO<sub>3</sub> orthoenstatite by Chopelas and Boehler (personal communication) showed a distinct change, between about 3.5 and 5 GPa, in the slopes of Raman frequencies with pressure,  $\delta\nu/\delta P$ . These observations suggested that orthoenstatite underwent a phase transition in this pressure interval, which could have a significant effect on its equation of state. We have therefore undertaken a high-pressure single-crystal X-ray diffraction study of end-member

TABLE 1. Variation of cell parameters with pressure

<i>P</i> (GPa)	<i>a</i> (Å)	<i>b</i> (Å)	<i>c</i> (Å)	<i>V</i> (Å <sup>3</sup> )
0.00	18.233(1)	8.8191(7)	5.1802(5)	833.0(1)
0.33	18.2143(9)	8.8105(8)	5.1735(5)	830.2(1)
0.75	18.1969(7)	8.7926(4)	5.1671(4)	826.74(8)
1.04	18.186(2)	8.782(1)	5.1610(6)	824.3(1)
1.28	18.1768(9)	8.7751(7)	5.1596(5)	823.0(1)
1.95	18.148(1)	8.756(1)	5.1493(7)	818.2(1)
2.19	18.1428(4)	8.7479(3)	5.1467(2)	816.84(5)
2.49	18.1280(5)	8.7381(4)	5.1418(2)	814.49(5)
2.82	18.1175(5)	8.7289(4)	5.1381(3)	812.56(6)
3.27	18.1045(6)	8.7181(4)	5.1327(3)	810.13(6)
3.64	18.0884(7)	8.708(1)	5.1280(6)	807.7(2)
3.88	18.0830(7)	8.7020(5)	5.1257(3)	806.57(7)
4.09	18.0710(7)	8.6929(5)	5.1214(3)	804.52(7)
4.26	18.065(2)	8.690(2)	5.119(1)	803.5(2)
4.52	18.063(1)	8.684(1)	5.1172(7)	802.7(1)
4.76	18.0526(9)	8.6770(8)	5.1145(5)	801.15(9)
4.98	18.0455(6)	8.6708(5)	5.1119(3)	799.86(6)
5.07	18.0409(8)	8.6696(6)	5.1106(4)	799.34(8)
5.13	18.037(1)	8.6686(9)	5.1102(6)	799.0(1)
5.37	18.027(2)	8.661(2)	5.1075(9)	797.4(2)
5.53	18.023(1)	8.658(1)	5.1052(6)	796.7(1)
5.85	18.011(2)	8.652(2)	5.102(1)	795.1(2)
6.36	18.007(2)	8.637(1)	5.0980(8)	792.9(2)
7.00	17.983(1)	8.6241(9)	5.0902(7)	789.4(1)
8.10	17.950(4)	8.604(5)	5.080(2)	784.5(5)
8.51	17.9361(8)	8.5897(6)	5.0760(5)	782.03(9)

MgSiO<sub>3</sub>, orthoenstatite to determine both its equation of state and the mechanisms of compression over the pressure range 0–8.5 GPa.

### EXPERIMENTAL DETAILS

A fragment measuring 125 × 50 × 30 μm was cut from a large synthetic MgSiO<sub>3</sub> orthoenstatite crystal (U.S. NMNH 137311). It was found to be free from twins and optical imperfections and was selected on the basis of X-ray diffraction peak profiles collected on a diffractometer. A data collection was carried out at room temperature and pressure with a conventional glass-fiber mount before the crystal was mounted in a modified Merrill-Bassett type diamond-anvil cell (Hazen and Finger, 1982). The crystal was later transferred to a DXR4 type diamond-anvil cell (Angel et al., 1992b) to obtain data at pressures exceeding 5.5 GPa. The pressure medium used was a 4:1 methanol-ethanol mixture, and pressure was determined by using the R<sub>1</sub> laser-induced fluorescence from a ruby chip included in the cell; the wavelength shift was converted to pressures using the calibration of Mao et al. (1986), and the precision of the pressure measurements is estimated to be better than ±0.03 GPa.

A Picker four-circle diffractometer equipped with a Mo X-ray tube (*K*α radiation obtained by β filtering) was used throughout the experiment. Unit cells were determined at each pressure by a vector least-squares fit (Ralph and Finger, 1982) to the positions of 28–32 accessible reflections in the range 12° < 2θ < 25° centered by the method of King and Finger (1979). Unit cells at all pressures displayed orthorhombic symmetry within the estimated standard deviations (esd); cell parameters obtained with orthorhombic constraints are reported in Table 1. Equations of state were fitted to the unit-cell data using a non-

TABLE 2. Refinement parameters

<i>P</i> (GPa)	Cell type	No. refs. before averaging	No. obs. <i>I</i> > 3σ <sub><i>i</i></sub>	<i>R</i> (av.)	<i>R</i> <sub><i>u</i></sub>	<i>R</i> <sub><i>w</i></sub>	<i>G</i> <sub><i>u</i></sub>
0.00	1	1232	681	0.0287	0.049	0.047	1.57
1.04	2	1235	642	0.036	0.058	0.055	1.44
1.95	1	1226	657	0.0315	0.074	0.066	1.85
3.27	1	1199	687	0.034	0.056	0.048	1.40
4.09	1	1268	723	0.031	0.064	0.056	1.69
4.95	1	1102	605	0.0331	0.074	0.069	1.83
5.85	2	1187	613	0.043	0.068	0.057	1.70
7.00	2	1121	668	0.045	0.056	0.060	1.32
8.10	2	1142	672	0.046	0.069	0.074	1.64

Note: cell type 1 refers to the Merrill-Bassett type diamond-anvil cell; cell type 2 refers to the DXR4 type cell.

linear least-squares refinement technique, refining the initial volume, *V*<sub>0</sub>, room-pressure bulk modulus, *K*<sub>0</sub>, and *K*'<sub>0</sub> simultaneously. Because a simple Murnaghan equation of state does not describe the data adequately at higher pressures, a Birch-Murnaghan third-order equation of state (Birch, 1947) was used throughout. A fourth-order Birch-Murnaghan equation of state gave no better fit to the data than a third-order equation of state, with *K*'' refining in all cases to less than its estimated standard deviation. The quality of fit of the various equations of state to the data were assessed by means of an *R* value, defined as

$$R = \frac{\sum |P_{\text{obs}} - P_{\text{calc}}|}{\sum |P_{\text{obs}}|}$$

Structural data of the compressed MgSiO<sub>3</sub> orthoenstatite were collected at pressure intervals of approximately 1 GPa. For these data collections, intensities of all accessible reflections to 2θ = 60° in one-half of reciprocal space were collected with ω scans of 1° total width and a step size of 0.025°, in a constant precision mode, to obtain *I*/σ<sub>*i*</sub> > 10, subject to the restriction of a maximum count time per step of 8 s. Room-pressure data from the crystal mounted in the cell containing no fluid was also collected to eliminate the possibility of systematic errors in the refined parameters arising from either restricted access to the reflections or uncertainties in the corrections for diamond-anvil cell absorption. Standard reflections were collected every 200 min to check for drift of the diffractometer and intensity decrease (for example, due to failure of the X-ray tube). No significant or systematic variations in these standard reflections were seen during the course of any data collection. Refinement parameters are given in Table 2.

Integrated intensities were obtained from the step scans by a modified Lehmann-Larsen algorithm (Grant and Gabe, 1978), with the option to reset backgrounds interactively. Much care was taken to ensure that only the Bragg intensity was integrated and any diffuse background excluded. Intensities were corrected for diamond absorption, Lorentz-polarization effects, shadowing by the gasket, and absorption by the crystal itself (typically, μ<sub>1</sub>

=  $10 \text{ cm}^{-1}$ ). The reflections were averaged in Laue group *mmm*. Refinements to structure factors with  $F > 6\sigma_F$  were carried out with the RFINE90 program, a development version of the RFINE4 program (Finger and Prince, 1975), with reflections assigned weights of  $\sigma^{-2}$ , where  $\sigma$  was derived from counting and averaging statistics. Positional parameters, bond lengths, and angles are given in Table 3.<sup>1</sup> All of the bond lengths in the room-pressure refinement are within 2 combined esd of the structure of  $\text{MgSiO}_3$  orthoenstatite reported by Ohashi (1984); most are within 1 esd.

## RESULTS

### Equations of state

Unit cells were determined at approximately 0.3-GPa intervals to 8.5 GPa. There were no observed hysteresis effects on increasing and decreasing the pressure, and no systematic differences between data collected in the two types of diamond-anvil cell. A single equation of state fitted to the entire data set has the parameters  $K_0 = 103.1(1.9)$  GPa,  $K'_0 = 9.2(0.6)$ , and  $R = 0.86\%$ . However, the systematic pattern of residuals ( $P_{\text{obs}} - P_{\text{calc}}$ ) indicates that this single equation of state is not an adequate description of the volume variation of the orthoenstatite with pressure. In fact, the data display a distinct discontinuity at a pressure of approximately 4 GPa. This discontinuity is reproducible and independent of the type of diamond-anvil cell employed for the diffraction experiment—note that the data points at 4.09 and 4.26 GPa are from different loadings of the crystal in two cells of different designs. The volume variation is better described by two separate equations of state fitted independently to the data at 0–4 and 4–8.5 GPa (Fig. 1):

$$P < 4 \text{ GPa} \quad K_0 = 95.8(3.0) \text{ GPa} \quad K'_0 = 14.9(2.0)$$

$$P > 4 \text{ GPa} \quad K_0 = 122.8(16.5) \text{ GPa} \quad K'_0 = 5.6(2.9)$$

The combined  $R$  value for this pair of equations of state is 0.71%, a significant improvement over the single equation of state at the 95% confidence level as assessed by a Hamilton test (Hamilton, 1965).

At 4 GPa, the difference in volume predicted by the two equations of state is  $0.7 \text{ \AA}^3$  per cell, which is on the order of the experimental uncertainties. We have attempted to determine whether this volume change is significant by refining two equations of state constrained to have the same volume at the crossover pressure  $P_{\text{cr}}$ . Free refinement of  $P_{\text{cr}}$  with the other equation of state parameters ( $V_0$ ,  $K_0$ , and  $K'_0$  for the low-pressure regime, and  $K_{P=P_{\text{cr}}}$  and  $K'_{P=P_{\text{cr}}}$  for the high-pressure regime) partially converges to  $P_{\text{cr}} = 4.27$  GPa and oscillates by  $\pm 0.03$  GPa about this value. The  $R$ -value of this fit is 0.86%, significantly worse than the two independent equations of state

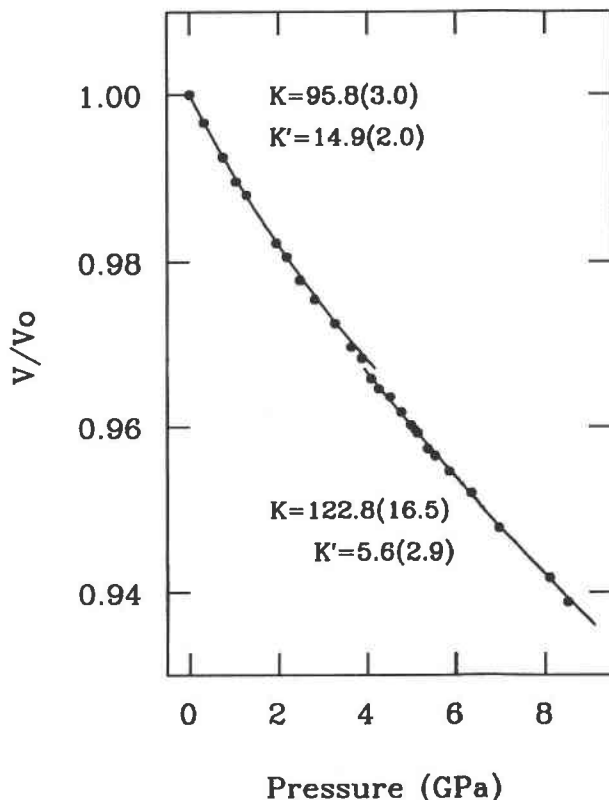


Fig. 1. The variation of the volume of orthoenstatite with pressure; uncertainties in  $V/V_0$  and the pressure are less than the size of the symbols. Note the distinct discontinuity in the volume at  $\sim 4$  GPa. The lines represent two third-order Birch-Murnaghan equations of state of  $\text{MgSiO}_3$  orthoenstatite fitted to the data, with the parameters shown. The numbers in parentheses represent standard deviations from the quoted values of  $K_0$  and  $K'_0$ .

at the 95% confidence level. Although these results are suggestive of the break in the equation of state being accompanied by a volume change, it must be remembered that the fundamental assumptions underlying the use of finite-strain equations of state are violated in such a case. The apparent volume change may therefore be an artifact, and we are unable to conclude whether the equation of state has a distinct break or whether there is a continuous crossover transition in the pressure interval  $\sim 3.9$ – $4.3$  GPa.

Determinations of the adiabatic bulk moduli of orthopyroxenes have been made at low and ambient pressures by Brillouin spectroscopy and ultrasonic techniques. Weidner et al. (1978) reported a room-pressure adiabatic bulk modulus ( $K_s$ ) of 107.8 GPa for  $\text{MgSiO}_3$ , which corresponds to an approximate value of  $K_0 [= K_s(1 + \alpha\gamma T)^{-1}]$  of 106.7 GPa. An equation of state fitted to our low-pressure data ( $P < 4$  GPa), with  $K_0$  fixed at this value gives  $V_0 = 832.4(1) \text{ \AA}^3$ ,  $K'_0 = 8.4(7)$ , and  $R = 1.5\%$ , a poor fit, with  $V_0$  differing from the observed value by  $> 4$  combined esd. Even allowing for uncertainties in the con-

<sup>1</sup> For a copy of Table 3 order Document AM-94-551 from the Business Office, Mineralogical Society of America, 1130 Seventeenth Street NW, Suite 330, Washington, DC 20036, U.S.A. Please remit \$5.00 for the microfiche.

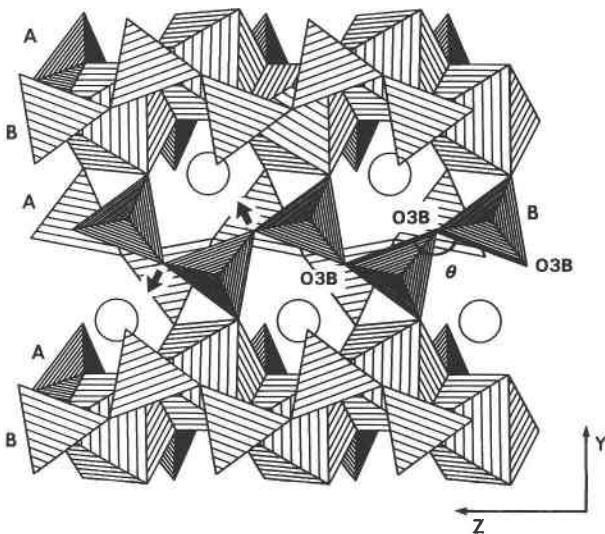


Fig. 2. A polyhedral representation of a portion of the orthoenstatite structure at 0 GPa, viewed down the  $x$  axis. M1 polyhedra are shown as octahedra, M2 sites as circles. The upper tetrahedral chains are all B chains, the lower ones are all A chains (Cameron and Papike, 1981). The chain extension angle,  $\theta$ , of the B chain is indicated. Arrows indicate the directions of movement of the O3B atoms on increasing pressure, which result in a decrease in the extension angle of the B chain and a decrease in M2-O3B distance.

version of adiabatic moduli to isothermal moduli due to the large uncertainties for orthopyroxenes in the factor  $(1 + \alpha\gamma T)$ , the value of  $K_0$  determined by Weidner et al. (1978) is inconsistent with our data. However, the large value of  $K'_0$  that we obtained in the low-pressure regime is confirmed by ultrasonic measurements of orthopyroxene to pressures of 3 GPa (Webb and Jackson, 1993). Detailed comparison with our data is difficult, not only because of the uncertainties in the adiabatic to isothermal conversion, but also because Webb and Jackson (1993) used a pyroxene containing about 20% Fe, which may cause a 1% decrease in bulk modulus from the value for pure enstatite (Weidner et al., 1978).

Calculation of the relative compressions of the axes (i.e.,  $a/a_0$ ) up to 8.5 GPa shows the [010] direction to be the most compressible and [100] the least. Two independent third-order Birch-Murnaghan equations of state were fitted to each of the axial shortenings; these exhibit a small but distinct break at about 4 GPa. In all three directions the higher pressure regime (with  $P > 4$  GPa) has higher moduli than the lower pressure regime, and the first derivatives of these moduli are approximately half the value of those at the lower pressure.

### Structure

Orthopyroxenes consist of alternating layers of  $\text{SiO}_4$  tetrahedra and  $\text{MgO}_6$  octahedra parallel to the (100) plane (Cameron and Papike, 1981). In each tetrahedral layer, the  $\text{SiO}_4$  tetrahedra share two corners with adjacent tet-

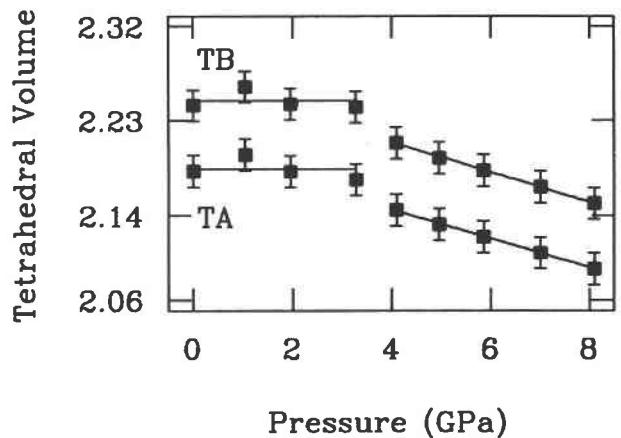


Fig. 3. Variation of average tetrahedral volume for both tetrahedra, with pressure. Note that the error bars represent the maximum uncertainty in the volumes; the standard deviations are less than these.

rahedra, forming infinite chains running parallel to the  $c$  axis. The more extended chain, as measured by the angle O3-O3-O3 (Fig. 2), with smaller tetrahedra, is referred to as the A chain, and the more kinked chain, with larger tetrahedra, is referred to as the B chain. The octahedral layer consists of two distinct M sites—a small, almost regular M1 site and a larger distorted M2 site.

The space group of orthoenstatite at ambient pressure is  $Pbca$ , although there have been some reports of orthopyroxenes exhibiting  $P2_1ca$  symmetry (e.g., Smyth, 1974; Harlow, 1980; Luo et al., 1992). It has been demonstrated that most examples of apparent  $P2_1ca$  symmetry (i.e., the observation of reflections violating the reflection condition  $k = 2n$  in  $0kl$ ) arise from a combination of exsolution textures and diffuse diffraction (Sasaki et al., 1984). Scans for intensity at the positions of systematic absences of the space group  $Pbca$  were therefore undertaken at 2.05 GPa. No reflections were observed with  $I > 3\sigma$ , confirming that the crystal used in our experiments has  $Pbca$  symmetry. A similar set of scans at 5.17 GPa also revealed no observed violations of  $Pbca$  symmetry, thus demonstrating that the change in compressional behavior at 4 GPa is not accompanied by any symmetry change.

Before now, Si-O bonds in pyroxenes have been considered to be essentially incompressible (Levien and Prewitt, 1981; Hazen and Finger, 1977), as Ralph and Ghose (1980) also demonstrated for orthoenstatite at pressures up to 2.1 GPa. However, although our data confirm this behavior (i.e., no significant change in either Si-O bond lengths or O-Si-O bond angles) at pressures below 4 GPa, there is considerable shortening of the Si-O bonds at higher pressures. Even above 4 GPa the O-Si-O bond angles remain unchanged within their estimated standard deviations, but the tetrahedral bond lengths decrease significantly, resulting in a very significant decrease in the volumes of the two  $\text{SiO}_4$  tetrahedra (Fig. 3). The linear compressibilities of the volumes ( $\beta_v$ ) of both of the

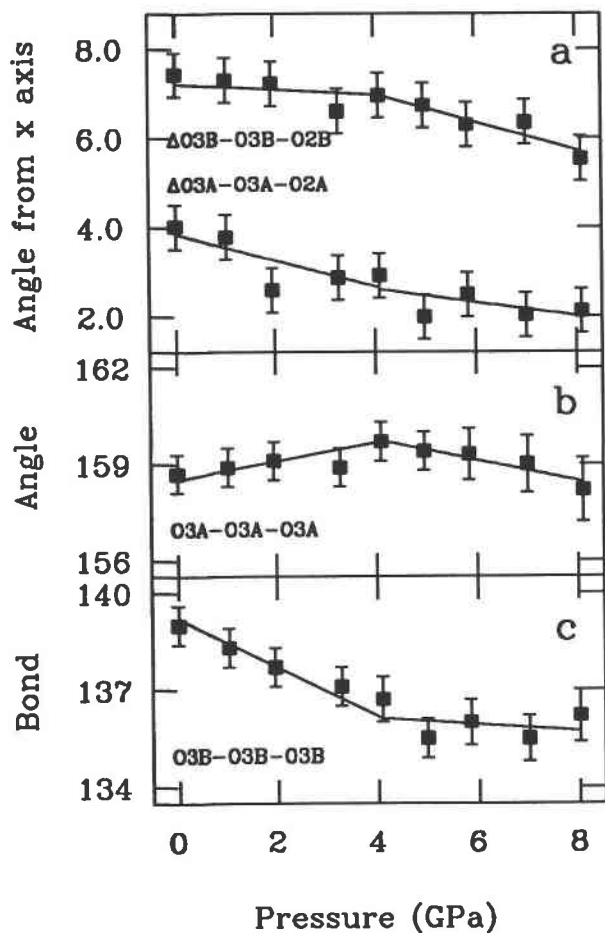


Fig. 4. (a) Angle of tilt of the tetrahedra in both chains with respect to the (100) plane. This tilt is determined as the angle between the normal to the basal plane of the tetrahedra (defined by coordinates of the O2 and O3 atoms), and the [100] direction. (b and c) Variation of the chain extension angle, O3-O3-O3, for the A and B chains. Note the change in slopes at 4 GPa.

$\text{SiO}_4$  tetrahedra above 4 GPa are  $0.0062(1) \text{ GPa}^{-1}$ , corresponding to bulk moduli of  $162(3) \text{ GPa}$ .

High-pressure studies of other silicate minerals have shown that  $\text{SiO}_4$  tetrahedra are generally incompressible over the pressure range of 0–~5 GPa. The few studies that have been performed at pressures significantly in excess of 5 GPa have, however, revealed compression of  $\text{SiO}_4$  tetrahedra that, as in orthoenstatite, is due to compression of the Si-O bonds rather than due to deformation (i.e., flattening) of the tetrahedra. The compressibility of the tetrahedra in orthoenstatite is intermediate between that in  $\text{Mg}_2\text{SiO}_4$  olivine, for which a  $\beta_v$  of  $0.0071(3) \text{ GPa}^{-1}$  can be calculated from the data to 14.9 GPa of Kudoh and Takéuchi (1985), and that in andradite to 19 GPa (Hazen and Finger, 1989), for which  $\beta_v = 0.0050(4) \text{ GPa}^{-1}$ .

Kinking of the tetrahedral chains, as measured by changes in the O3-O3-O3 chain extension angle (Fig. 2), also occurs in an irregular way over the whole pressure

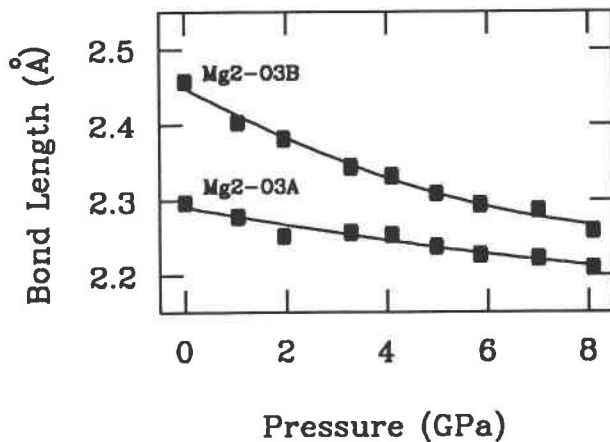


Fig. 5. Compression of the Mg2-O3 bonds up to 8 GPa. The standard deviation of the pressure is considerably less than the width of the symbols.

range studied. Up to 4 GPa, the B chain, which is the more distorted at room pressure, kinks dramatically, keeping the bases of its tetrahedra at a constant orientation of approximately  $7^\circ$  from the (100) plane (Fig. 4). Above 4 GPa, the kinking ceases, and the tetrahedra begin to tilt steadily toward the (100) plane. The A chain behaves in essentially the reverse way; below 4 GPa, the tetrahedra tilt markedly toward the (100) plane with only a little chain kinking occurring, whereas at higher pressures the tetrahedral tilt virtually stops and the kinking continues slowly, but in the opposite direction (Fig. 4).

Compression of the Mg octahedra is intimately connected with the deformation of the tetrahedral chains through the sharing of O atoms. It is therefore somewhat surprising that we find that compression of the Mg octahedra occurs in a continuous manner, with no apparent discontinuity in either the rate of bond shortening or polyhedral compression at 4 GPa. All the Mg-O bonds decrease steadily in length, although the Mg2-O3 bonds compress more dramatically than the rest (Fig. 5; also Ralph and Ghose, 1980). The octahedral volumes are seen to decrease in a similarly regular way. This compression is described by a single third-order Birch-Murnaghan equation of state for each octahedron:

$$\text{M1 site} \quad K_0 = 53.2(5.4) \text{ GPa} \quad K'_0 = 31.9(6.3)$$

$$\text{M2 site} \quad K_0 = 63.1(8.5) \text{ GPa} \quad K'_0 = 26.7(7.9).$$

The octahedra, which make up approximately 23% of the total volume of the structure, are thus more compressible than the structure as a whole.

## DISCUSSION

By collecting high-precision structural data at closely spaced pressure intervals, we have demonstrated that orthoenstatite undergoes a change in compression mechanisms at ~4 GPa. At lower pressures compression is accommodated by changes in the conformation of the chains

of essentially rigid  $\text{SiO}_4$  tetrahedra, but above 4 GPa there is in addition significant compression of the Si-O tetrahedral bonds. This change in compression mechanism is reflected in the equation of state of orthoenstatite, which shows a distinct break at this pressure (Fig. 1), and it is also apparent in a change in the rate of change,  $\delta\nu/\delta P$ , of the Raman frequencies of enstatite between 3.5 and 5 GPa (Chopelas and Boehler, personal communication).

It is not clear from the data in the literature whether such changes in compression mechanism are a general phenomenon but have not usually been observed because of insufficient data coverage or insufficient precision in high-pressure structure refinements. Alternatively, these kinds of change may only occur in structures in which there are sufficient degrees of freedom within the structure to allow smooth compression of the polyhedra of the larger cations independently or semi-independently of discontinuous changes in the compression of the silicate tetrahedra. We do note that  $\text{MgSiO}_3$  orthorhombic perovskite with  $\text{SiO}_6$  octahedra also shows a change in compression mechanism at 5 GPa (Ross and Hazen, 1990).

Our results on orthoenstatite generally confirm the proposals of Webb and Jackson (1993) that the compression of the deformed M2 octahedra should eventually reach a stage where further kinking of the tetrahedral chains becomes energetically unfavorable. As this situation is approached, they expect the pressure derivatives of the moduli to return to normal values (i.e., comparable with those observed for simple structures). That is what we have observed:  $K'_0$  decreases from 14.9 to 5.6 at a pressure of 4 GPa, where the change in compression mechanism occurs. The high value of  $K'_0$  at low pressure is therefore attributed to the initial rapid compression of the Mg2-O3B bond, which requires the concomitant changes in the conformation of the tetrahedral B chain.

#### ACKNOWLEDGMENTS

We would like to thank A. Chopelas for drawing our attention to the anomalous behavior of orthoenstatite at high pressure and for providing the crystals used in this study. We are grateful to J.R. Smyth, L.W. Finger, and C.T. Prewitt for thought-provoking reviews of the manuscript. R.J.A. wishes to thank the Royal Society for its support in the form of a 1983 University Research Fellowship, and D.A.H.-J. acknowledges the receipt of Research Studentship GT4/4/92/223 from the Natural Environment Research Council (NERC). High-pressure diffraction experiments at UCL are supported by research grants from NERC (grant GR3/369) and the Royal Society.

#### REFERENCES CITED

- Angel, R.J., Chopelas, A., and Ross, N.L. (1992a) Stability of high-density clinoenstatite at upper-mantle pressures. *Nature*, 358, 322–324.
- Angel, R.J., Ross, N.L., Wood, I.G., and Woods, P.A. (1992b) Single-crystal X-ray diffraction at high pressures with diamond-anvil cells. *Phase Transitions*, 39, 13–32.
- Birch, F. (1947) Finite elastic strain of cubic crystals. *Physical Review*, 71, 809–824.
- Cameron, M., and Papike, J.J. (1981) Structural and chemical variations in pyroxenes. *American Mineralogist*, 66, 1–50.
- Finger, L.W., and Prince, E. (1975) A system of Fortran IV computer programs for crystal structure computations. U.S. National Bureau of Standards Technical Note, 854, 128 p.
- Gasparik, T. (1989) Transformation of enstatite-diopside-jadeite pyroxenes to garnet. *Contributions to Mineralogy and Petrology*, 102, 389–405.
- Grant, D.F., and Gabe, E.J. (1978) The analysis of single-crystal Bragg reflections from profile measurements. *Journal of Applied Crystallography*, 11, 114–120.
- Hamilton, W.C. (1965) Significance tests on the crystallographic R-factor. *Acta Crystallographica*, 18, 502–510.
- Harlow, G.E. (1980) Low orthopyroxene: Achondritic abundance and planetary significance. *Lunar and Planetary Science*, 11, 396–397.
- Hazen, R.M., and Finger, L.W. (1977) Compressibility and structure of Angra dos Reis fassaite. *Carnegie Institution of Washington Year Book*, 76, 512–515.
- (1982) Comparative crystal chemistry, p. 28–38. Wiley, New York.
- (1989) High-pressure crystal chemistry of andradite and pyrope: Revised procedures for high-pressure diffraction experiments. *American Mineralogist*, 74, 352–359.
- Kanzaki, M. (1991) Ortho/clinoenstatite transition. *Physics and Chemistry of Minerals*, 17, 726–730.
- King, H., and Finger, L.W. (1979) Diffracted beam crystal centering and its application to high-pressure crystallography. *Journal of Applied Crystallography*, 12, 374–378.
- Kudoh, Y., and Takéuchi, K. (1985) The crystal structure of forsterite  $\text{Mg}_2\text{SiO}_4$  under high pressure up to 149 kbar. *Zeitschrift für Kristallographie*, 171, 291–302.
- Levien, L., and Prewitt, C.T. (1981) High-pressure structural study of diopside. *American Mineralogist*, 66, 315–323.
- Luo, G., Xue, J., Xu, H., Xu, H., and Hu, M. (1992) Confirmation of the terrestrial occurrence of orthopyroxene with space group  $P2_1ca$ . *American Mineralogist*, 77, 115–120.
- Mao, H.K., Xu, J., and Bell, P.M. (1986) Calibration of the ruby pressure gauge to 800 kbar under quasi-hydrostatic conditions. *Journal of Geophysical Research*, 91, 4673–4676.
- Ohashi, Y. (1984) Polysynthetically-twinned structures of enstatite and wollastonite. *Physics and Chemistry of Minerals*, 10, 217–229.
- Pacalo, R.E.G., and Gasparik, T. (1990) Reversals of the orthoenstatite-clinoenstatite transition at high pressures and high temperatures. *Journal of Geophysical Research*, 95, 15853–15858.
- Ralph, R.L., and Finger, L.W. (1982) A computer program for refinement of crystal orientation matrix and lattice constants from diffractometer data with lattice symmetry constraints. *Journal of Applied Crystallography*, 15, 537–539.
- Ralph, R.L., and Ghose, S. (1980) Enstatite,  $\text{Mg}_2\text{SiO}_6$ : Compressibility and crystal structure at 21 kbar (abs.). *Eos*, 61, 409.
- Ross, N.L., and Hazen, R.M. (1990) High-pressure crystal chemistry of  $\text{MgSiO}_3$  perovskite. *Physics and Chemistry of Minerals*, 17, 228–237.
- Sasaki, S., Prewitt, C.T., and Harlow, G.E. (1984) Alternative interpretation of diffraction patterns attributed to low ( $P2_1ca$ ) orthopyroxene. *American Mineralogist*, 69, 1082–1089.
- Smyth, J.R. (1974) Low orthopyroxene from a lunar deep crustal rock: A new pyroxene polymorph of space group  $P2_1ca$ . *Geophysical Research Letters*, 1, 27–29.
- Webb, S.L., and Jackson, I. (1993) The pressure dependence of the elastic moduli of single-crystal orthopyroxene ( $\text{Mg}_{0.8}\text{Fe}_{0.2}\text{SiO}_3$ ). *European Journal of Mineralogy*, 5, 1111–1119.
- Weidner, D.J., Wang, H., and Ito, J. (1978) Elasticity of orthoenstatite. *Physics of the Earth and Planetary Interiors*, 17, 7–13.

MANUSCRIPT RECEIVED AUGUST 18, 1993

MANUSCRIPT ACCEPTED DECEMBER 30, 1993